

Femtosecond time-resolved molecular multiphoton ionization and fragmentation of Na_2 : experiment and quantum mechanical calculations

V. Engel, T. Baumert, Ch. Meier, G. Gerber

Fakultät für Physik, Albert-Ludwigs-Universität, Hermann-Herder-Strasse 3, D-79104 Freiburg, Germany

Received: 22 February 1993 / Final version: 22 April 1993

Abstract. We present a comparison between experimental and theoretical results for pump/probe multiphoton ionizing transitions of the sodium dimer, initiated by femtosecond laser pulses. It is shown that the motion of vibrational wave packets in two electronic states is probed simultaneously and their dynamics is reflected in the total Na_2^+ ion signal which is recorded as a function of the time delay between pump and probe pulse. The time dependent quantum calculations demonstrate that two ionization pathways leading to the same final states of the molecular ion exist: one gives an oscillating contribution to the ion signal, the other yields a constant background. From additional measurements of the Na^+ -transient photofragmentation spectrum it is deduced that another ionization process leading to different final ionic states exists. The process includes the excitation of a doubly excited bound Rydberg state. This conclusion is supported by the theoretical simulation.

PACS: 33.80.Eh; 33.10. – n

1. Introduction

Traditionally spectroscopy is performed in the frequency domain: transitions between atomic or molecular eigenstates are induced by the absorption of nearly monochromatic radiation from a light source. By changing the frequency of the radiation the absorption spectrum as a function of energy is detected. Quantum beat spectroscopy is an alternative way to study the spectral properties of atoms [1] and molecules [2]. The experiments are carried out in the time domain: a laser light pulse is employed which is able to excite two or more energy states of the atom (or molecule) coherently. Afterwards the fluorescence from the excited states is monitored and the Fourier transform of the temporal beat signal yields the energy level spacings of the system.

In the last years it became possible to detect atomic radial motion [3, 4] and the vibrations of small molecules

in real time [5, 6]. Because of the intrinsic timescales of the systems ultrashort laser pulses are required to obtain temporal resolution. In the case of the atomic “Rydberg wave packets” [7] ps laser pulses are able to prepare a coherent superposition of radial wave functions. To detect molecular vibrations it is necessary to use fs laser pulses which are readily available. A typical experimental set up consists of a pump/probe arrangement: a femtosecond pump laser pulse whose spectral width is broad enough to excite several eigenstates of the system under consideration prepares a localized wave packet. This evolves in time and is probed with a second time delayed laser pulse which interacts with the sample of molecules at different delay times. An electronically excited state is prepared which afterwards decays radiatively. Then, if appropriate wavelengths are employed, the total fluorescence measured as a function of delay time shows the underlying dynamics. Alternatively one may ionize the molecule with the probe pulse and a transient ionization spectrum taken as a function of delay time between pump and probe pulse yields the dynamical information.

Recently a time resolved study of the femtosecond multiphoton ionization of Na_2 has been reported [8, 9]. From the data the authors deduced that molecular bound state motion in two different electronic states was probed in the experiment. Furthermore the basic problem of competing mechanisms like direct ionization, autoionization and autoionization induced fragmentation was discussed.

In what follows we will distinguish between *ionization pathways* and *ionization processes*. This is important in the interpretation of our experiment. In Fig. 1 we illustrate two ionization schemes (α) and (β) for a pump/probe multiphoton transition. The horizontal lines indicate electronic states of the molecule and the boxes represent the manifold of accessible vibrational ionic states which are reached if electrons with different translational energies are ejected. In the case (α) one photon is absorbed from the pump pulse and two photons are absorbed from the probe pulse, leading to ions in a set of final states. (β) represents the situation where two

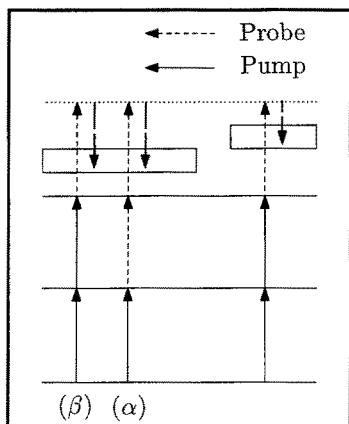


Fig. 1. Ionization pathways and ionization processes in a multi-photon ionization. Electronic states of a molecule are shown as horizontal lines. The two boxes stand for the two different sets of final ionic vibrational states which are accessible in the experiment. The downward arrows indicate the electrons released with kinetic energies E_{kin} in the ionization processes. The excitation by absorption of photons from pump and probe pulses is indicated by the upward arrows

photons are absorbed from the pump pulse and one photon from the probe. In both cases the same set of final ionic states are reached thus (α) and (β) are two different ionization pathways. The amplitudes for the pathways have to be added coherently. Contrarily, an excitation scheme which leads to different final states of the ion represents a different ionization process. This situation is sketched in the right part of Fig. 1. The amplitudes for different ionization processes add incoherently.

In this paper we want to compare the previous analysis with the results of a time dependent, quantum mechanical calculation. It will be shown that the calculation can reproduce the experimental findings in any respect. There are only a few theoretical studies of femtosecond ionization processes involving several electronic states of a molecule [10–12]. The present case of the sodium dimer presents a challenge for the theory and one can hope to learn more about what happens during the absorption of many photons by a molecule on the femtosecond time scale.

The paper is organized as follows: Section 2 contains a brief description of the experimental set up. In Sect. 3 we give the results of the measurements and discuss different ionization pathways and processes. The theoretical model and calculations for the ionization pathways are presented in Sect. 4. Theory and experiment are compared in Sect. 5 and we summarize the paper in Sect. 6.

2. Experimental

The experimental set up is described in detail elsewhere [8]. Here we briefly outline the techniques which have been employed. Femtosecond laser pulses induce and probe the molecular transitions. A supersonic molecular beam provides vibrational and rotational cold Na_2 molecules in a collision-free environment in the electronic

ground state $X^1\Sigma_g^+$. Time-of-flight (TOF) spectroscopy is employed to determine the kinetic energy of the electrons, the mass of the ions and the released kinetic energy of the ionic fragments.

The molecular beam is produced either by a pure sodium expansion or by an expansion seeded with Argon. The oven is usually operated at 1000 K with nozzle temperatures about 50 K higher. Due to the cooling effect of the supersonic expansion the vibrational level $v''=0$ in the $X^1\Sigma_g^+$ ground state of Na_2 is predominantly populated. The laser-molecular beam interaction region is placed between parallel plates so that the formed ions and electrons can be detected in opposite directions by two differently designed TOF-spectrometers arranged perpendicular to the laser and molecular beam. Femtosecond laser pulses are generated in a home-built colliding-pulse mode-locked (CPM) ring dye laser following the design of Valdmanis and Fork [13]. Pulses of 60 fs duration at the center wavelengths of 627 nm are produced. We obtain CPM output pulses with an average power of 15 mW in a 75 MHz pulse train. The spectral distribution of the output pulses is measured with an optical multichannel analyzer. The pulse duration is determined by the autocorrelation technique using non-collinear second harmonic generation [14]. The spectral distribution and the time duration of the CPM pulses are monitored during the experiment. Since the CPM pulse energies are much too low (≈ 0.2 nJ) for our molecular beam experiment, we employed dye amplifiers pumped at a rate of 100 Hz by a synchronized 308 nm excimer laser to increase the pulse energies to a level suited for the chosen experiment. A Michelson arrangement was used to delay the probe laser relative to the pump laser. Both the pump and the probe laser enter the interaction region collinearly with the same polarization and perpendicular to the molecular beam. For the experiments we have used recompressed laser pulses of 70–80 fs time duration; about 100 Å spectral width and of 0.2 μJ energy ($I \approx 50$ GW/cm²) for both the pump and the probe. The laser pulse energy was kept this low in the pump-probe experiment to simplify the study of the basic physical processes (see discussion below). Using this intensity the average ion signal produced by the pump or the probe pulse alone is reduced to less than 10%. By setting the gate of a boxcar integrator to a specific ion time-of-flight, dimer ions or ionic Na^+ fragments are detected. Each data point is obtained by averaging over 1000 pump-probe experiments while the delay time is scanned over 20 fs. By this data acquisition we detect the wave packet dynamics by means of the transient ion spectra. Furthermore we avoid to resolve the interferometric structures reflecting the period of the optical cycle of our laser which are induced by coherent interaction of pump and probe laser pulses. This is in contrast to the work of Scherer et al. [15] who, in their experiments intentionally controlled the relative phase between pump and probe pulses.

3. Experimental results and discussion

In the present experiments we are interested in the dynamics of molecular multiphoton ionization and fragmentation on a femtosecond time scale. Three photons of our laser wavelength are needed to ionize the Na_2 molecule in a multiphoton process. The first time-resolved studies of molecular multiphoton ionization in a molecular beam using femtosecond pump-probe techniques [16] revealed unexpected features of the dynamics which takes place during the absorption of many photons by a diatomic molecule.

3.1. The transient Na_2^+ spectrum

The observed femtosecond pump-probe delay spectrum, i.e. the transient Na_2^+ ionization spectrum is shown in Fig. 2. The ion signal exhibits a beat structure superimposed on a strong modulation and a constant background. Because pump and probe are identical the signal is symmetric around zero time delay. The modulation period estimated from the peak to peak separation is $T = 306$ fs. Evident from the beat structure in Fig. 2, there are at least two oscillating contributions to the transient ionization spectrum and the envelope intensity variation reveals them to be about 180° out of phase. Two temporal oscillations with a zero phase difference will exhibit a maximum at time $t = 0$. On the other hand, a phase difference of 180° results in an envelope variation with a minimum value at $t = 0$ and increasing values for increasing times as is seen in Fig. 2. That the signal nevertheless exhibits a maximum at zero delay time is due to the fact that pump and probe pulse overlap. In this case the molecule interacts with an electric field of doubled amplitude which results in a strongly enhanced ion signal. The strong modulation of the ionization signal decreases for longer delay times.

The periodic variation of the ion signal and the superimposed modulation suggests that wave packet motions in molecular bound states are probed in our exper-

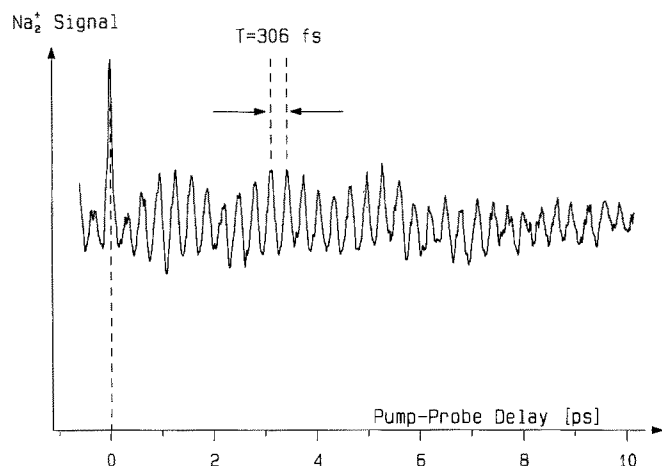


Fig. 2. Transient Na_2^+ signal obtained as a function of Pump-Probe delay time between two identical femtosecond laser pulses

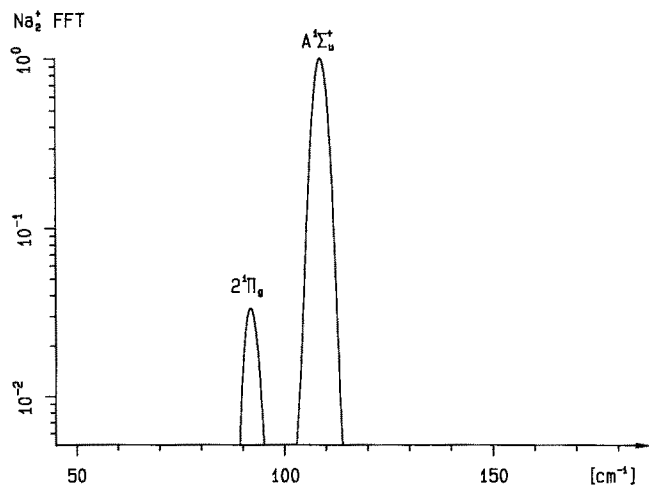


Fig. 3. Fourier spectrum of the transient Na_2^+ signal displayed in Fig. 2

iment. Wave packet motions have already been seen in pump/probe fluorescence experiments on other diatomic systems [15, 17–22]. The 306 fs separation of the peaks points towards vibrational motion of the Na_2 molecule. Since we use laserpulses with a spectral width which is broad compared to the vibrational level spacing Δv in electronic states of Na_2 accessible in our experiment, localized vibrational wave packets can be prepared. In general, molecular potentials are not purely harmonic so that a vibrational wave packet will disperse after some time. This dispersion may cause the observed signal to decrease for longer delay times just as it is seen in Fig. 2. The spreading and recurrence of the vibrational wave packet for long delay times has been described in a recent study [23]. Here we are interested in the details of the basic excitation, ionization and fragmentation processes which can be extracted from the time dependence of the ion signals at short delay times.

In order to derive the frequency components of the pump-probe delay spectrum a Fourier analysis was performed and the result is displayed in Fig. 3. The power spectrum density shows two major groups of frequencies, one centered at 108.7 cm^{-1} , the other centered at 92.0 cm^{-1} . The individual frequencies are unresolved due to the limited scan length of the pump-probe spectrum. From the Na_2^+ ionization spectrum and its Fourier transform we identify two major contributions to the multiphoton ionization of Na_2 . They will be discussed separately in what follows.

3.2. Wave packet motion in the $A(^1\Sigma_u^+)$ -state

The Na_2 molecules in the ground state $^1\Sigma_g^+$ and $v'' = 0$, J'' are pumped into excited electronic states by a laser pulse, whose 70–80 fs duration is much shorter than the vibrational period of Na_2 . For a center wavelength of 627 nm and a bandwidth of about 10 nm the vibrational levels $v' = 10$ –14 are coherently excited by the fs pulse so that a wave packet is formed in the electronic $A^1\Sigma_u^+$ state. The corresponding level spacings are 109.5, 108.8, 108.1

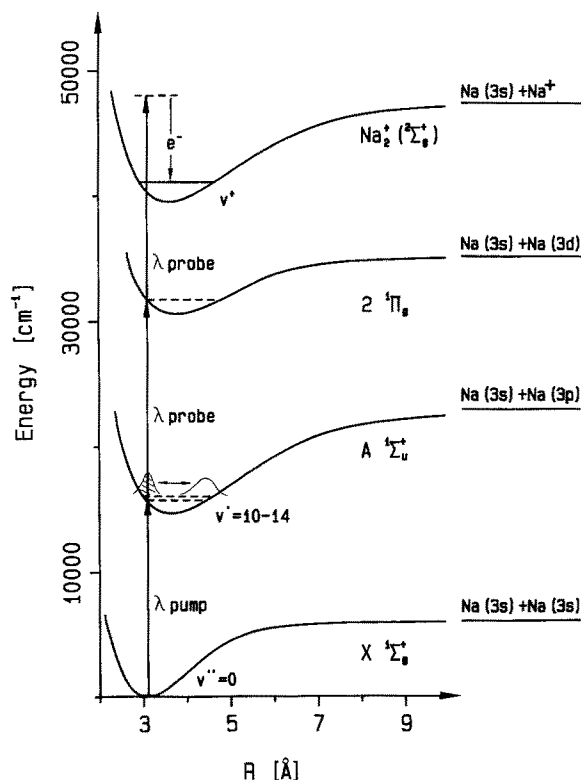


Fig. 4. Scheme for a one photon pump and two photon probe direct ionization. The potential energy curves for the involved electronic states are drawn. The pump pulse prepares a coherent superposition of the vibrational states $v' = 10-14$ in the electronic A -state. The motion of the vibrational wave packet is probed by a time delayed second femtosecond laser pulse

and 107.4 cm^{-1} [24], respectively. These values agree with one of the frequency components derived from the Fourier analysis. The averaged classical vibrational period for these levels is around 306 fs, in agreement with the separation of the large amplitude peaks in the transient ion signal of Fig. 2. The shape of the wave packet depends on the amplitudes of the components, which are determined by the pump laser spectral distribution and the Franck-Condon factors of the involved transitions. Starting initially only from the $v'' = 0$ vibrational ground state, the packet originates at the inner turning point of the A -state potential (see Fig. 4).

The motion of the wave packet in the A -state potential is probed after a variable time delay T . The 70 fs probe pulse ionizes the molecule in a transition involving the intermediate $2^1\Pi_g(3s, 3d)$ Rydberg state. From the oscillatory Na_2^+ signal (period 306 fs), which is in phase with the preparation of the wave packet at the inner turning point at time $t=0$, the A -state motion is evidently probed only near the inner turning point. Probing at the outer turning point would result in a 180° phase shift, which is not observed. Note that a direct non resonant two-photon transition from the A -state into the Na_2^+ ionization continuum will result in a time independent ionization signal, because the shapes of the two potentials are so similar [25]. Analysis based on the difference potentials between the ionic ground $X^2\Sigma_g^+$, $A^1\Sigma_u^+$ and $2^1\Pi_g$

states shows that only through the resonant intermediate Π -state, which acts as a “window” for the two photon probe transition, the motion of the A -state wave packet can be seen. In fact the difference potential shows, that the Π -state restricts the possible transitions to a region close to the inner turning point [8].

Figure 4 summarizes the results described in this section. It contains the relevant potential curves and indicates the preparation and probing of the A -state wave packet. The packet is prepared in the A -state at the inner turning point (or more precisely at the inner turning point which belongs to the mean excitation energy) and is probed every time it recurs in the spatial region around that distance.

3.3. Wave packet motion in the $2^1\Pi_g$ -state

The Fourier analysis (Fig. 3) of the Na_2^+ ionization signal and the observed beat structure (Fig. 2) imply a second major ionization channel. This ionization channel is connected with an “out of phase” wave packet motion as mentioned in Sect. 3.1. Based on the derived Fourier component of about 92 cm^{-1} and the femtosecond laser wavelengths of 627 nm, we conclude that the pump laser creates a coherent superposition of vibrational levels in the Π -state via a two photon transition. The absorption of two laser photons induces transitions from the $v'' = 0$ level in the electronic ground state to vibrational levels between the $v^* = 11$ to $v^* = 18$ in the Π -state. Using the known spectroscopic constants [26, 27] the vibrational spacings can be calculated. They range from 89.7 to 94.1 cm^{-1} and agree with the frequencies obtained from the Fourier analysis (Fig. 3). The vibrational wave packet in the Π -state is also formed close to the inner turning point of the respective potential (see Fig. 6). The one-photon probe process detects the real time motion of the packet but only, as the phase shift of 180° clearly shows, at delay times when the packet is localized near the outer turning point of its motion. We just described a multiphoton ionization process where first two pump photons are absorbed and a vibrational wave packet is built at short bond distances but is probed at the earliest time after half of the v^* vibrational period of about 175–185 fs, that is when the maximum vibrational stretch is assumed. This gives rise to a periodic variation of the ion signal. From Franck-Condon arguments one can deduce that the ionization probability does not depend upon where the wave packet is located in the Π -state potential. Moreover, the difference potential analysis applied to the $2^1\Pi_g \rightarrow \text{ion } X(^2\Sigma_g^+)$ probe transition [8] and also wave packet calculations [25] show that direct photoionization out of the Π -state results in a time independent total ionization signal. This will add a time independent signal to the total ion signal. So far it is not obvious why the ionization out of the Π -state takes preferentially place at the outer turning point as it is deduced from our measurements. Possible explanations for the observed phase shifted wave packet contribution in the transient Na_2^+ signal could be

- A transition dipole moment that strongly increases with increasing internuclear distances

- Stimulated emission pumping during the probe laser duration, that occurs only at the inner turning point of the Π -state potential. This process decreases the ion yield. The loss due to stimulated emission down to the A -state is only possible if the wave packet is located close to the inner turning point. This follows from Franck-Condon arguments [8].
- Another independent ionization process, different from direct photo-ionization of a singly excited electronic state and enhanced at delay times when the wave packet reaches the outer turning point in the Π -state potential.

3.4. The transient photofragmentation spectrum

In order to gain more insight into the existence of a “second” ionization process, we have performed another time-resolved experiment where the variation of the Na^+ ionic photofragment signal as a function of the delay time between the femtosecond pump and probe laser pulses was measured. The TOF-analysis shows that the ionic fragments have a small kinetic energy corresponding to the absorption of three photons from pump and probe pulse together. This is important for the conclusions presented below. Figure 5 compares the transient spectra for Na^+ and Na_2^+ obtained from measurements under the same experimental conditions. The oscillation period of the transient Na^+ fragmentation spectrum is determined by the wave packet motion in the Π -state, as an analysis based on the laser parameters for this experiment shows. Moreover, it again shows the phase shift of 180° with respect to zero delay time. The results of this time-resolved photofragmentation experiment strongly suggest that the Na^+ ionic fragments with small kinetic energy W and the molecular ions which are formed via a one photon probe transition from the Π -state if the respective wave packet is located around the outer turning point, have a common origin.

The excitation of the inner electron of the Na_2 ($3s$, $3d$) Rydberg state by the probe laser into a higher orbital $n'l'$, to form a neutral electronically doubly excited molecule, is such a process. The decay channels of a bound

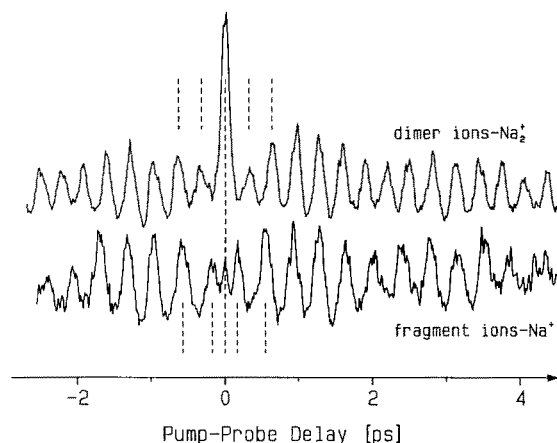
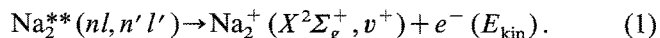


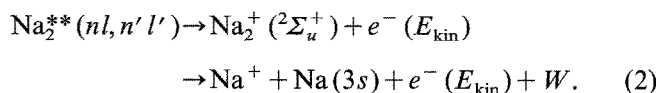
Fig. 5. Comparison of the transient Na_2^+ ionization and Na^+ photofragmentation spectra obtained under the same experimental conditions

doubly excited molecule $\text{Na}_2^{**}(nl, n'l')$ can account for the identical structure in the transient Na_2^+ ionization and in the Na^+ photofragmentation spectra. These channels, relevant to the observed spectra are:

- Electronic autoionization, responsible for the observation of the phase shifted Π -state wave packet motion in the Na_2^+ ionization spectrum:



- Autoionization induced fragmentation, responsible for the observation of the phase shifted Π -state wave packet motion in the Na^+ photofragmentation spectrum:



Reasons why such a “core”-excitation occurs preferentially at the outer turning point of the Π -state could be the relative location of the involved potentials or a strong R -dependence of the transition dipole moment. Preliminary calculations of bound doubly excited Na_2^{**} potential energy curves by Meyer [28] show (for a $^1\Pi_u$ state) the required relative location of the two involved potential curves.

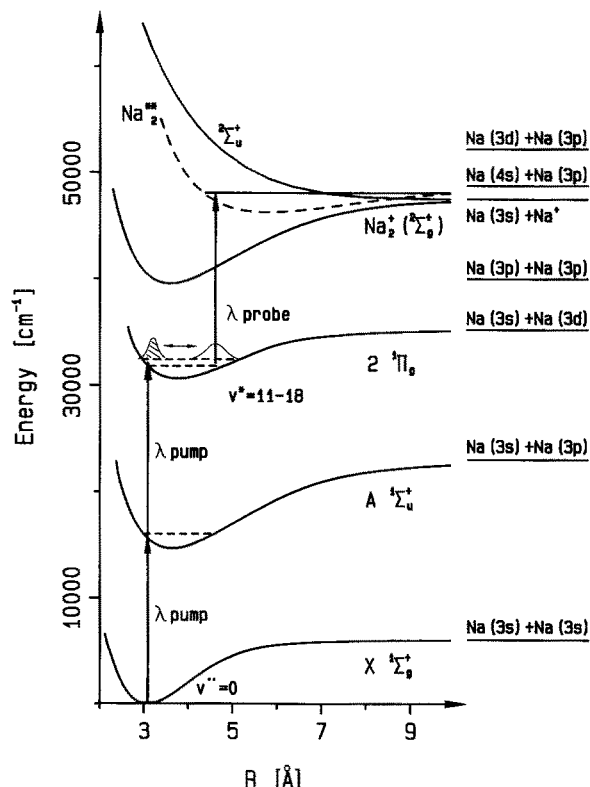


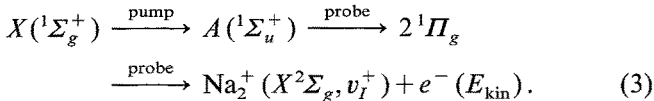
Fig. 6. Ionization scheme for a two photon pump transition to the electronic Π -state and an indirect one photon ionization which proceeds via a doubly excited Rydberg-state and electronic autoionization. This explains the modulation of the Na_2^+ signal due to its Π -state component and the characteristic oscillation of the transient spectrum of slow ionic fragments

The two-photon pump and one-photon probe ionization process which involves excitation and decay of a doubly excited state is illustrated in Fig. 6. Except for the repulsive ${}^2\Sigma_u^+$ state [29] and the estimated Na_2^{**} curve, all other curves are RKR potentials. In a two photon transition the pump laser prepares a wave packet at the inner turning point, which then propagates in about 180 fs to the outer turning point where the probe laser transfers the motion into the continuum by exciting a second electron forming bound doubly excited Na_2^{**} molecules. From the observed ion and electron spectra [8, 16], these molecules have different ionization and fragmentation channels compared to direct photoionization and bound-free fragmentation. What we have just described is indeed another ionization process (see Fig. 1): the electron spectra reveal that ions are built within vibrational states v_I^+ which are not accessible by direct photoionization out of the Π -state [8].

3.5. Summary of the experimental results

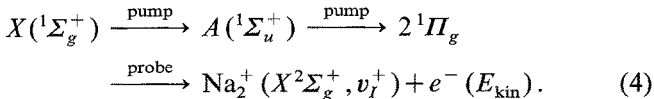
On the basis of a) an analysis of the transient Na_2^+ ionization spectrum, b) an analysis of the transient Na^+ photofragmentation spectrum and c) a difference potential analysis [8] we conclude that in our experiment molecular sodium ions are produced not only by direct photoionization of singly excited electronic states but also through an independent second multiphoton process involving the excitation of a doubly excited molecular Rydberg state $\text{Na}_2^{**}(nl, n' l')$ and a decay via electronic autoionization and autoionization induced fragmentation. In detail we have:

1. One contribution which consists of the direct photoionization of a singly excited electronic state

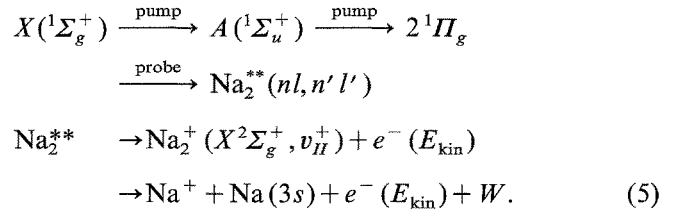


This one photon pump and two photon probe process occurs at the inner turning point of the A -state potential with the periodicity of the motion of the respective vibrational wave packet.

2. A second contribution obtained by a two photon pump and one photon probe transition which accounts for the time independent signal in our measurements.



Molecular ions are built in the same vibrational states v_I^+ which are populated in the first ionization pathway. 3. The third contribution involves a bound doubly excited neutral electronic state which decays subsequently through electronic autoionization and autoionization induced fragmentation (Fig. 6)



This two photon pump and one photon probe process occurs only through probe excitation at the outer turning point of the Π -state, the first time at a delay of ≈ 180 fs between pump and probe laser pulse. The final vibrational states of the ions v_{II}^+ are different from the states v_I^+ .

4. Theory

4.1. The model

We use time dependent perturbation theory up to third order to describe the pump/probe experiments discussed above. The total Na_2^+ population as a function of the delay time between the pump and probe pulse is calculated. Four electronic states are incorporated in our study. The corresponding potential energy curves, taken from [24, 26, 30, 31] are drawn in Fig. 4. In what follows we will drop the detailed spectroscopic assignments and refer to the electronic X -, A -, Π -states of the sodium dimer and the ionic ground state of Na_2^+ .

Direct three photon ionization processes are not included. We checked numerically that the corresponding transition probabilities are negligible. The wave packet propagation is done with the split-operator-technique [32, 33] and the time integrals of the perturbation theory were calculated as outlined in [34]. Throughout the numerical calculation we used Gaussians with a width (FWHM) of 80 fs for the pulse envelopes. The center wavelength was set to 627 nm. Since the experiments are performed in a molecular beam we take the vibrational ground state within the electronic X -state as the initial wave function. The rotational degree of freedom is not included since for short decay times it does not play a significant role.

To describe the ionization we discretized the ionization continuum. In what follows we will separately describe the two ionization pathways as it was done in the Sects. 3.2. and 3.3. Section 4.4 contains a discussion of the coherent sum of the two indistinguishable pathways leading to sodium dimer ions in the same set of final states. This strategy enables us to see how much a quantum mechanical calculation can reproduce what has been deduced from the experimental results.

4.2. Quantum dynamics in the electronic A -state

As indicated in Fig. 4, a pump pulse with a central wavelength of 627 nm can induce a transition from the ground to the electronic A -state. We describe the pump process with first order time dependent perturbation theory. Within this approximation the wave function in the A -state can be written as [35] ($\hbar = 1$)

$$|\psi(t), A\rangle \sim \int_0^t dt' U_A(t-t') W_{AX}(t', \omega) U_X(t') |\psi_0, X\rangle. \quad (6)$$

Here $U_A(t)$, $U_X(t)$ represent the time evolution operators in the respective electronic states and the initial state $|\psi_0, X\rangle$ is the vibrational ground state of energy E_i . The light-matter interaction is chosen to be

$$W_{AX}(t, \omega) = -\mu_{AX} E_0 e^{-i\omega t} f(t), \quad (7)$$

where μ_{AX} is the projection of the $X-A$ transition dipole moment on the polarization vector of the electric field of strength E_0 and frequency ω . The dipole moment is taken to be independent of the internuclear distance, i.e. we employ the Condon-approximation. $f(t)$ is the envelope function of the laser pulse which is taken to be a Gaussian centered at a large enough time so that it vanishes at the origin $t=0$.

The pump pulse prepares a wave packet in the A -state, consisting of a linear combination of vibrational eigenfunctions. Once the pulse stops the packet propagates unperturbed and periodically back and forth. A study of the long time behaviour can be found in [23]. For short time (some picoseconds) its motion is almost classical and spatially restricted by the classical turning points in the A -state potential which correspond to the mean excitation energy of 627 nm. This behaviour is illustrated in Fig. 7. In the upper panel we plot the A -state potential and wave packets at the three intermediate times $t=80, 328$ and 555 fs. The lower part contains the expectation value

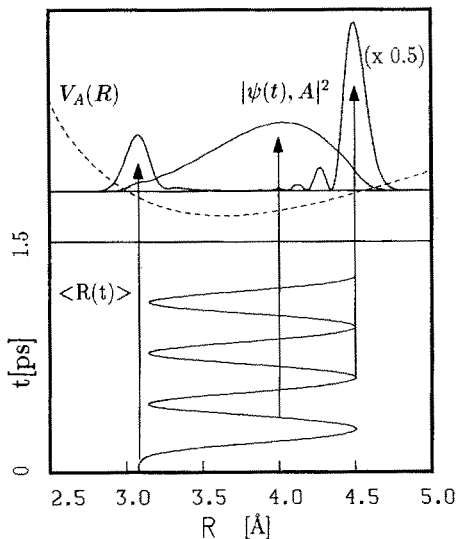


Fig. 7. *Upper panel:* The potential for the electronic A -state is shown as a dashed curve. The intersection of the horizontal line with the potential marks the classical turning point which correspond to the mean energy of the wave packet. Wave functions $|\langle R | \psi(t, A) \rangle|^2$ (6) are shown for different times. *Lower panel:* the coordinate expectation value (8) calculated with the moving A -state wave packet. The arrows mark the times at which the wave functions in the upper panel are drawn

$$\langle R(t) \rangle = \langle \psi(t), A | R | \psi(t), A \rangle / \langle \psi(t), A | \psi(t), A \rangle. \quad (8)$$

The expectation value reflects the oscillatory motion of the wave packet (period = 305 fs) between the two classical turning points R_{\pm} defined by $V_A(R_{\pm}) = E_i + \omega$. The time $t=80$ fs corresponds to the center of our Gaussian envelope function $f(t)$ for the pump pulse. From Fig. 7 it is evident that the wave packet in the A -state is created around the inner turning point of the respective potential. The question is if the dynamics of the wave packet can be seen in the Na_2^+ ion signal. Since the ions are built via a two photon transition second order perturbation theory has to be applied to calculate the ion yield. The total ionic wave function can be written as

$$|\psi_{\alpha}(t)\rangle = \int_0^{E_{\max}} dE' |\psi_{\alpha}(t), E' + \rangle. \quad (9)$$

The integral appears because the ionization continuum is accessed and electrons with kinetic energy E' up to a maximal energy E_{\max} can be ejected. $|E' + \rangle$ denotes the electronic wave function of the free and the bound electrons. Since the states of the free electron are orthonormal for different energies E' the total electronic wave functions are orthonormal as well. The index α was added to specify the particular ionization pathway which is the topic of this subsection. The vibrational wave functions are calculated with the second order formula

$$|\psi_{\alpha}(t), E' + \rangle \sim \int_0^t dt'' U_{+}(t-t'') W_{+\pi}(t'', \omega - E') \times \int_0^{t''} dt' U_{\pi}(t''-t') W_{\pi A}(t', \omega) |\psi(t'), A\rangle. \quad (10)$$

Here $U_{+}(t)$ and $U_{\Pi}(t)$ denote the time evolution operators in the ionic ground- and Π -state. The interactions W_{nm} are the same as in (7) since we adopt the Condon approximation and furthermore assume that the ionization cross section does not depend on the energy E' [36]. We have discretized the continuum, i.e. the integral in (8) is replaced by a sum over discrete energies E' . It was found that an energy grid with a stepsize of 0.02 eV between $\omega - E' = 1.02$ eV and 1.28 eV gave converged results. The rather large stepsize expresses the fact, that the distribution of the Franck-Condon factors for vibrational transitions between the Π - and ionic state change smoothly over the energy interval. The restricted energy range is due to the Franck-Condon factors between the vibrational wave functions of the ionic ground and lower lying electronic states. The wave functions $|\psi_{\alpha}(t), E' + \rangle$ depend on the delay time between pump and probe pulse which is not indicated explicitly in the equations. The partial ionic populations have been calculated for different values of $\omega - E'$ and different delay times T :

$$P_{\alpha}(T, E') = \lim_{t \rightarrow \infty} \langle \psi_{\alpha}(t), E' + | \psi_{\alpha}(t), E' + \rangle. \quad (11)$$

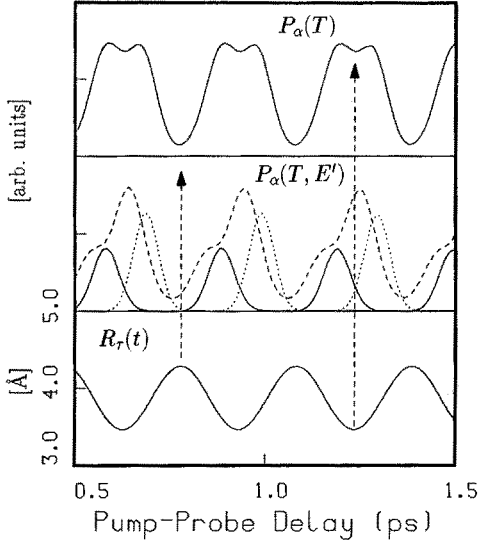


Fig. 8. *Upper panel:* Total ion population prepared by a two photon ionization process out of the electronic A -state as a function of delay time between pump and probe pulse. *Middle panel:* Partial ion signals (11) for energies of 1.04 eV (straight line), 1.1 eV (dashed line) and 1.16 eV (dotted line). The curves are drawn on a larger scale than the total ion signal. *Lower panel:* Expectation value for the bond length in the A -state (12), averaged over the length of the probe laser pulse

These populations correspond to the fraction of ions which are built by the ejection of an electron with translational energy E' . The limit in (11) is obtained when the probe pulse decays to zero since then the population remains constant.

Results for representative energies are displayed in Fig. 8 as a function of the delay time T between the pump and probe laser pulse. We also plot the sum of the partial signals, i.e. the total ion signal $P_\alpha(T)$. Simultaneously the expectation value of the bond length in the A -state, averaged over the length τ of the probe laser pulse is shown:

$$R_\tau(t) = \frac{1}{\tau} \int_{t-\tau/2}^{t+\tau/2} dt \frac{\langle \psi(t), A | R | \psi(t), A \rangle}{\langle \psi(t), A | \psi(t), A \rangle}. \quad (12)$$

This quantity measures the average position of the A -state wave packet during the interaction with the probe pulse, i.e. it shows us “where” the packet is probed during its motion [37]. It would be misleading to consider the expectation value of (8) since the packet moves during the probe process. Several conclusions can be drawn from the figure:

- the vibrational period ($T=305$ fs) of the wave packet motion is reflected in the partial as well as in the total ion signal.
- ions are predominantly built at delay times when the wave packet is close to the inner turning point of the A -state potential.
- There is no one-to-one correspondence between the location of the wave packet and a maximum in the partial ion signal. Rather, the occurrence of a maximum depends on the direction of the motion of the wave packet.

The first two conclusions are in agreement with what has been deduced from a potential difference analysis [8]: the ionization proceeds via the intermediate II -state and resonant A - II -transitions are only allowed at small bond lengths. Thus the II -state acts as a filter and only a small amount of ions are built if the wave packet is at the outer turning point of the A -state potential.

The third conclusion cannot be explained without taking the dynamics of the wave packet into account. For a two photon transition it is not only the A - II difference potential but also the II -ionic difference potential which is important in the resonance of resonant excitation. Assume that, according to the Franck-Condon principle, the classical transition point R_1 between A - and II -state, defined by

$$V_{II}(R_1) - V_A(R_1) = \omega \quad (13)$$

is smaller than a transition point R_2 between II and ionic state. If the wave packet is probed while it is moving from R_1 towards R_2 , then a resonant two photon transition takes place. On the other hand if it is moving from R_1 towards smaller distances, a transition to the ionic ground state is not possible. This is different from previously discussed one photon transitions where, in principle, a peak in the transition probability is obtained at any time the wave packet passes the transition point. A reminiscence of the effect shows up in the signal for 1.1 eV (dashed line in the middle panel of Fig. 8). It is curious that the latter effect seems to be visible in the time dependence of the total ion signal. However, the doublet on top of each maximum in the population is due to the summation over all partial ion signals which themselves do not show this splitting. We note that the splitting is very sensitive to small variations of the laser parameters.

4.3. Quantum dynamics in the electronic II -state

In Sect. 3.3 it was discussed, that the pump pulse can populate the II -state via a two photon transition from the ground state (see Fig. 6). The corresponding wave function is given in second order perturbation theory by

$$\begin{aligned} |\psi(t), II\rangle & \\ & \sim \int_0^t dt'' U_{II}(t-t'') W_{IIA}(t'', \omega) \\ & \times \int_0^{t''} dt' U_A(t''-t') W_{AX}(t', \omega) |\psi_0(t'), X\rangle. \end{aligned} \quad (14)$$

This vibrational wave packet moves periodically between the classical turning points of the II -state potential energy curve. Here we find a vibrational period of 360 fs. The total ionic wave function corresponding to a one photon probe process originating from the II -state (labeled by the index β) is given by:

$$|\psi_\beta(t)\rangle = \int_0^{E_{\max}} dE' |\psi_\beta(t), E' + \rangle. \quad (15)$$

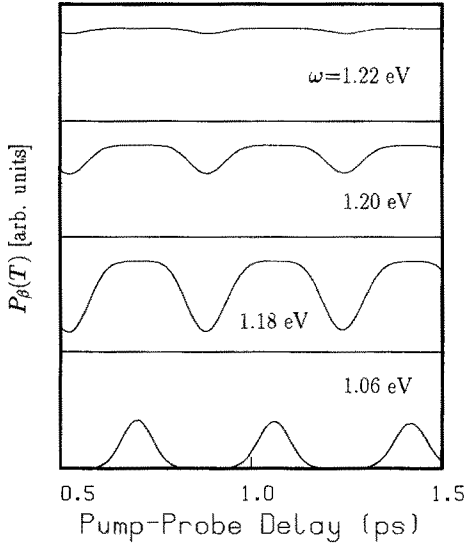


Fig. 9. Total ion signal obtained by a one photon direct ionization process initiating in the electronic Π -state for different central energies of the ionizing laser pulse. The pump laser energy was 627 nm

The energy dependent ionic vibrational wave functions are

$$|\psi_{\beta}(t), E' + \rangle \sim \int_0^t dt' U_+(t-t') \times W_{+\Pi}(t', \omega - E') |\psi(t'), \Pi\rangle. \quad (16)$$

With this wave functions one may calculate partial ion signals $P_{\beta}(T, E')$ (see (11)). It has been shown previously that the total ion signal obtained by a one photon transition from the Π -state does not depend on the delay time between pump and probe pulse [8, 25] (see also [11]). One of the reasons for this effect is that for a diatomic molecule (with some exceptions) the potentials for electronically excited states and the ionic ground state show a similar dependence on the internuclear distance. Furthermore it is due to the Condon-approximation which ignores the coordinate dependence of the transition dipole moment and to the wavelength of the ionizing laser (627 nm) which does not restrict the final vibrational states which are accessible. How a time independent ion signal arises is demonstrated in Fig. 9. The different panels contain the *total* ionic populations calculated with different probe laser energies ω , as indicated. For a small energy (1.06 eV) only lower vibrational states of the ion are accessible. The signal is periodic (360 fs) and reflects the wave packet dynamic in the Π -state. With increasing energy more vibrational ionic states are populated and the time dependence is lost. For $\omega = 1.977$ eV, which corresponds to the experimental wavelength of 627 nm, one does not observe a dependence of the ion signal on the delay time between pump and probe pulse. Ions are created no matter where the wave packet is located when the probe pulse interacts with the molecule. This is due to the fact that with increasing probe energy more and more ionic final states are accessed. The calculations may be summarized as follows:

- The partial ion signals reflect the periodicity of the Π -state vibrational motion with a period of 360 fs.
- The total ion signal does not depend on the delay time between pump and probe pulse.

4.4. The coherent sum of the ion signals and summary of the theoretical results

In the preceding sections we have discussed separately two different pathways, leading to the same set of final ionic states via a three photon pump/probe scheme. Since the experiment cannot distinguish how the Na_2^+ ions are built it is necessary to consider the coherent sum of the amplitudes for the different processes. Summing up the total ionic wavefunctions of (9) and (15) one obtains the population

$$P(T) = \langle \psi_{\alpha} | \psi_{\alpha} \rangle + \langle \psi_{\beta} | \psi_{\beta} \rangle + 2 \text{Re} \langle \psi_{\alpha} | \psi_{\beta} \rangle = P_{\alpha}(T) + P_{\beta}(T) + P_{\alpha\beta}(T). \quad (17)$$

Here the explicit time dependence of the wave functions has been dropped, meaning that we regard any time when the probe pulse has passed through the sample and the populations have become constant. $P(T)$ consists of three terms: $P_{\alpha}(T)$ and $P_{\beta}(T)$ represent the incoherent contributions of the two pathways as discussed in Sect. 4.2. and 4.3., respectively. According to what has been found P_{α} will oscillate with a period of 305 fs and P_{β} gives a time independent signal. $P_{\alpha\beta}$ is an interference term resulting from the coherent superposition of the two ionization pathways α and β .

Identical and time delayed pump and probe laser pulses are produced by means of a Michelson interferometer in the experiment so that the electric field of pump and probe laser can be written as

$$E(t) = f_1(t) e^{-i\omega t} + f_2(t-T) e^{-i\omega(t-T)}. \quad (18)$$

The use of the field in this form in the theoretical description assumes that experimental phase fluctuations from shot to shot can be neglected. This was verified experimentally [38] but it is not important for the following discussion. Within our theoretical model the interference term $P_{\alpha\beta}(T)$ oscillates with $\cos(\omega T)$. If the measured (or calculated) signal is averaged over several optical cycles the interference contribution vanishes. Since the experiment was performed to find the envelope of the transient ion signal an average was performed as discussed in Sect. 2. We thus neglect the term $P_{\alpha\beta}(T)$ for the comparison with the experiment.

Altogether the quantum mechanical calculation performed within the present model has shown that the total ion signal obtained from direct photoionization can be separated into two contributions. The first shows a periodic time dependence which reflects the motion of the vibrational wave packet in the electronic A -state. The motion of another wave packet in the Π -state is not seen in the total ion signal [25]. The contribution from the Π -state leads to a time independent signal. Since the interference term is not resolved in the present experi-

ment, the two contributions simply add to the total ionic population.

5. Comparison between experimental and theoretical results

We now turn to a comparison between the experimental and theoretical results, keeping in mind that the theoretical model is restricted to direct photoionization only. Figure 10 contains the measured Na_2^+ signal (upper panel) and the calculated ionic population $P_\alpha + P_\beta$ (lower panel) as a function of delay time between pump and probe pulse. The pronounced oscillations with the A -state vibrational period are present in both curves and occur at the same delay times. As noted above this curve shows only the A -state periodic wave packet motion. Furthermore the time independent part of the experimental signal is higher than in the calculation. Indeed there is another state ($4^1\Sigma_g^+$ [39]) which participates in the ionization [38]. The *direct* photoionization out of this state yields as well a time independent signal [40] and adds to the time independent signal.

To reproduce the experimental findings one has to postulate a process which will introduce the periodicity of the Π -state motion into the signal. In principle one may imagine three possibilities for such a process. The first is stimulated emission from the Π -down to the A -state. This is only possible if the wavepacket is located at the inner turning point of the Π -state potential and would yield the time dependence of the ion signal as seen in the experiment. Non perturbative calculations show that stimulated emission plays a significant role only if strong laser fields are used [41]. However for the intensities employed in the present experiment this process is negligible.

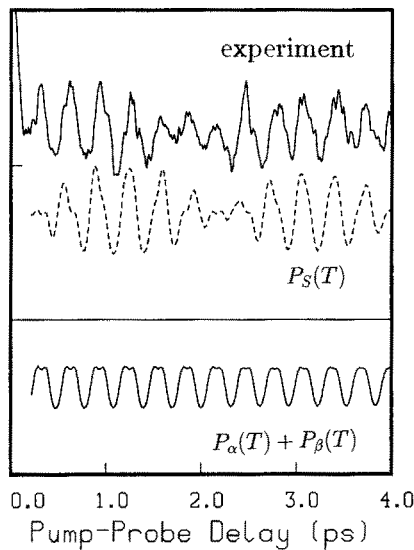


Fig. 10. The lower panel contains the incoherent sum of the calculated total ion signals P_α and P_β . Upper panel: Comparison between the measured transient ion signal and the simulated calculated signal P_S (19)

Another possibility is that the transition dipole moment for the Π -ionic transition shows a significant dependence on the interatomic distance R [25]. However, the comparison between Franck-Condon calculations and the results of nanosecond experiments shows that this is very unlikely [42]. Finally there might be another ionization pathway or process from the Π -state which preferentially takes place from the outer turning point of the corresponding potential. The experiment shows that there is such an ionization process leading to different ionic vibrational states. It was concluded [8, 16] that a doubly excited Rydberg state is involved (see Sect. 3). To simulate this findings we have calculated the population

$$P_S(T) = P_\alpha(T) + P_\beta(T) + \sum_{E'} P_\beta(T, E'), \quad (19)$$

which adds certain partial ion signals obtained by one photon ionization out of the Π -state to the sum of the total ionization signals P_α and P_β . As discussed above, the coherent contribution is not considered here because it was not resolved in the current experiment. In particular we added partial signals which lead to higher vibrational ionic states ($\omega - E' = 1.20, 1.22$ and 1.24 eV). These are obtained when the wave packet is close to the right hand turning point [25]. The results are displayed in the upper panel of Fig. 10 (dashed line) together with the measured total ion signal. A nearly perfect agreement is obtained. The strong A -state oscillations and the weak modulation of the peaks due to the Π -state dynamics is reproduced in the calculated curves.

6. Summary

In the present paper we have investigated the pump/probe multiphoton ionization of Na_2 . The total Na_2^+ signal as a function of delay time between pump and probe pulse was measured. The data showed two periodic contributions on top of a time independent signal. The strongest modulation belongs to the vibrational period of the electronic $A^1\Sigma_u^+$ state which is probed by a direct two photon ionization. The other is introduced via an indirect photoionization process involving a doubly excited Rydberg state ($\text{Na}_2^{**}(nl, n'l')$). Ions are produced by a one photon excitation from the $^1\Pi_g$ -state and subsequent electronic autoionization at delay times when the corresponding wave packet is close to its right hand turning point.

We have presented perturbative time dependent quantum calculations for direct photoionization from the electronic and vibrational ground state. The calculated signal for a one photon pump and two photon probe transition shows strong oscillations which are due to the wave packet motion in the A -state. The two photon pump and one photon probe ionization on the other hand leads to a signal which does not depend on the delay time between pump and probe pulse. Both ionization pathways lead to the same set of final vibrational states of Na_2^+ . Since the present experiment does not resolve interference contributions, the total ionic population consists of the sum of populations obtained from both pathways. This sum

shows only the periodicity of the A -state wave packet motion shifted by a time independent signal. To introduce a time dependence due to the I -state motion we added contributions which are obtained if the I -state wave packet is close to the outer turning point. This is consistent with what has been deduced from the experiment. The simulated curve shows a very good agreement with the measured ion signal, which strongly supports the conclusion that another process participates in the multiphoton ionization of Na_2 . This ionization process leads to a different set of final vibrational states of the ion which cannot be populated by direct photoionization. From the comparison between theory and experiment we have learned about the dynamics which takes place during the complicated multiphoton excitation of the sodium dimer. In the future we will extend the theoretical description to a non perturbative treatment [43]. First experimental and theoretical results have already been obtained [41]. Furthermore it will be interesting to include the doubly excited electronic state which will soon be available [28].

Financial support by the Deutsche Forschungsgemeinschaft within the SFB 276, "Korrelierte Dynamik hochangeregter atomarer und molekularer Systeme" is acknowledged. We thank G. Alber, J.S. Briggs and H.S. Taylor for stimulating discussions.

References

- Andrä, H.J.: In: Atomic physics, Vol. 4. zu Putlitz, G., Weber, E.W., Winnacker, A. (eds.). New York: Plenum Press 1975
- Hack, E., Huber, J.R.: *Int. Rev. Phys. Chem.* **10**, 287 (1991)
- Wolde, A. ten, Noordam, L.D., Lagendijk, A., van Linden van den Heuvell, H.B.: *Phys. Rev. A* **40**, 485 (1989)
- Yeazell, J.A., Mallalieu, M., Stroud, C.R.: *Phys. Rev. Lett.* **64**, 2007 (1990)
- Khundkar, L.R., Zewail, A.H.: *Ann. Rev. Phys. Chem.* **41**, 15 (1990)
- Zewail, A., Bernstein, R.: In: The chemical bond. Zewail, A. (ed.). San Diego: Academic Press 1992
- Alber, G., Zoller, P.: *Phys. Rep.* **199**, 231 (1991)
- Baumert, T., Bühler, B., Grosser, M., Weiss, V., Wiedenmann, E., Gerber, G.: *J. Phys. Chem.* **95**, 8103 (1991)
- Baumert, T., Grosser, M., Thalweiser, R., Gerber, G.: *Phys. Rev. Lett.* **67**, 3753 (1991)
- Engel, V., Metiu, H.: *Chem. Phys. Lett.* **155**, 77 (1989)
- Seel, M., Domcke, W.: *Chem. Phys.* **151**, 59 (1991)
- Seel, M., Domcke, W.: *J. Chem. Phys.* **95**, 7806 (1991)
- Valdmanis, J.A., Fork, R.L.: *IEEE J. Quantum Electron.* **22**, 112 (1986)
- Ippen, E.P., Shank, C.V.: In: Ultrafast light pulses. Shapiro, S.L. (ed.). Berlin, Heidelberg, New York: Springer 1977
- Scherer, N.F., Carlson, R.J., Matro, A., Du, M., Ruggiero, A.J., Romero-Rochin, V., Cina, J.A., Fleming, G.R., Rice, S.A.: *J. Chem. Phys.* **95**, 1487 (1991)
- Baumert, T., Bühler, B., Thalweiser, R., Gerber, G.: *Phys. Rev. Lett.* **64**, 733 (1990)
- Bowman, R.M., Dantus, M., Zewail, A.H.: *Chem. Phys. Lett.* **161**, 297 (1989)
- Janssen, M.H.M., Bowman, R.M., Zewail, A.H.: *Chem. Phys. Lett.* **172**, 99 (1991)
- Dantus, M., Bowman, R.M., Zewail, A.H.: *Nature* **343**, 737 (1990)
- Misewich, J., Glowonia, J.H., Rothenberg, J.E., Sorokin, P.P.: *Chem. Phys. Lett.* **150**, 374 (1988)
- Glowonia, J.H., Misewich, J., Sorokin, P.P.: *J. Chem. Phys.* **92**, 3335 (1990)
- Walkup, R.E., Misewich, J., Glowonia, J.H., Sorokin, P.P.: *Phys. Rev. Lett.* **65**, 2366 (1990)
- Baumert, T., Engel, V., Röttgermann, C., Strunz, W.T., Gerber, G.: *Chem. Phys. Lett.* **191**, 639 (1992)
- Gerber, G., Möller, R.: *Chem. Phys. Lett.* **113**, 546 (1985)
- Engel, V.: *Chem. Phys. Lett.* **178**, 130 (1991)
- Taylor, A.J., Jones, K.M., Schawlow, A.L.: *J. Opt. Soc. Am.* **A73**, 994 (1983)
- Whang, T.J., Wang, H., Li Li, Lyyra, A.M., Stwalley, W.C.: *J. Mol. Spectrosc.* **145**, 112 (1991)
- Meyer, W.: Privat communication
- Müller, W., Meyer, W.: *J. Chem. Phys.* **80**, 3311 (1984)
- Kusch, P., Hessel, M.M.: *J. Chem. Phys.* **68**, 2591 (1978)
- Bordas, C., Labastie, P., Chevaleyre, J., Broyer, M.: *Chem. Phys.* **129**, 21 (1989)
- Fleck, J.A., Morris, J.R., Feit, M.D.: *Appl. Phys.* **10**, 129 (1976)
- Feit, M.D., Fleck, J.A., Steiger, A.: *J. Comput. Phys.* **47**, 412 (1982)
- Engel, V.: *Comput. Phys. Commun.* **63**, 228 (1991)
- Loudon, R.: *The quantum theory of light*. Oxford: Clarendon Press 1983
- Chupka, W.A.: In: Ion-molecule reactions, Vol. 1, Franklin, J.L. (ed.). London: Butterworths 1972
- Engel, V., Metiu, H.: *J. Chem. Phys.* **93**, 5693 (1990)
- Baumert, T.: Thesis, University of Freiburg, 1992
- Wang, H., Whang, T.J., Lyyra, A.M., Li Li, Stwalley, W.C.: *J. Chem. Phys.* **94**, 4756 (1991)
- Engel, V.: (unpublished)
- Baumert, T., Meier, Ch., Gerber, G., Engel, V.: *Chem. Phys. Lett.* **200**, 488 (1992)
- Bühler, B.: Thesis, University of Freiburg, 1991
- Meier, Ch., Engel, V.: (to be published)